RSC Advances

PAPER

Cite this: *RSC Adv.*, 2022, **12**, 36115

Non-medicinal parts of safflower (bud and stem) mediated sustainable green synthesis of silver nanoparticles under ultrasonication: optimization, characterization, antioxidant, antibacterial and anticancer potential†

Simin Wei,[a] Mengke Hao,[a] Zhishu Tang,*[a] Tuan Zhou,[a] Fei Zhao[b] and Yinghui Wang*[c]

The flower of safflower is widely used in Chinese herbal preparations and the non-medicinal parts have been applied to develop a sustainable green method, where AgNPs were generated using a mixture of leaf and stem after 12 h of incubation in the dark. In this study, we intend to improve the efficiency of the reduction reaction and optimize this green method by selecting other non-medicinal parts, such as the bud and the pure stem, evaluating the biosynthesis parameters and harnessing the assistance of ultrasonication. Visual observation and UV-vis spectroscopy confirmed that both safflower stem (SS) and bud (SB) mediated AgNPs (SS-AgNPs and SB-AgNPs, respectively) could be produced rapidly over time under ultrasonication. An alkaline solution could accelerate the formation of SS-AgNPs and SB-AgNPs with greater surface loads. SS-AgNPs and SB-AgNPs of small size could be obtained at pH 8.0 and 10.0, respectively. Large concentrations of SS and SB extract are also beneficial for forming AgNPs of small size. It is in acid and neutral solutions that monodispersed SS-AgNPs and SB-AgNPs can be generated. Characterization of selectively synthesized SS-AgNPs and SB-AgNPs demonstrated their spherical shape with the actual size below 30 nm covered by anions. Both SS-AgNPs and SB-AgNPs exhibited potent antioxidant and antibacterial activity. The MIC values of SS-AgNPs for *S. aureus* and *E. coli* were 12.5 and 25.0 μg mL^{-1}, respectively, slightly superior to SB-AgNPs. In an *in vitro* anticancer assay, both kinds of AgNPs show potent toxicity action against the SW620 cell line with IC_{50} values of 5.4 and 10.6 μg mL^{-1}, respectively. However, only SS-AgNPs reveal an inhibitory action against the HeLa cell line, where the IC_{50} is found to be 26.8 μg mL^{-1}. These results provide experimental proof that the assistance of ultrasonication and adjusting the process parameters are efficient methods for promoting the reduction reaction, and both SS and SB mediated AgNPs could serve as a promising antioxidant, antibacterial and anticancer agents.

Received 11th October 2022
Accepted 5th December 2022

DOI: 10.1039/d2ra06414f

rsc.li/rsc-advances

1. Introduction

Silver nanoparticles (AgNPs) have aroused wide interest due to their remarkable and unusual chemical, biological and physical properties, and usually comprise 20–15 000 silver atoms of a size smaller than 100 nm.[1] Recently, AgNPs have been applied in the fields of biomedicine, pharmaceuticals, cosmetics, catalysis, textiles and optics.[2–14] Studies have documented that AgNPs could be physically or chemically synthesized with high yield, but physical methods require harsh conditions like high temperature, vacuum conditions, and sophisticated instruments, and chemical additives are necessary in chemical methods.[15–19] Obviously, these methodologies have high production costs or they may introduce toxic and dangerous chemicals, which have potential biological risks for the environment and health.[20,21] To alleviate these concerns, researchers have turned their attention to the green synthesis of AgNPs by bio-resources like plant extracts, bacteria, fungi and biopolymers, where the toxic substances are replaced by molecules included in these resources.[22–26] Among these methodologies, plant extracts are generally adopted more frequently as

[a]*State Key Laboratory of Research & Development of Characteristic Qin Medicine Resources (Cultivation), Co-Construction Collaborative Innovation Center for Chinese Medicine Resources Industrialization by Shaanxi & Education Ministry, Shaanxi University of Chinese Medicine, Xianyang 712083, China. E-mail: tzs6565@163.com*

[b]*College of Basic Medical Sciences, Shaanxi University of Chinese Medicine, Xianyang 712046, China*

[c]*College of Science, Chang'an University, Xi'an 710064, China. E-mail: wangyinghui@chd.edu.cn*

† Electronic supplementary information (ESI) available. See DOI: https://doi.org/10.1039/d2ra06414f

they can easily be improved, are less bio-threatening and do not include the step of cell culture growth.[27–29] Studies have confirmed that bioactive molecules in plant extracts, like flavonoids, polyphenols, proteins, sugars and saponins, could act as both reducing and capping agents.[25] Although the low toxicity of such plant extracts is satisfactory, the most exciting thing is the synergistic effect between bioactive molecules and AgNPs.[30,31] Therefore, the synthesis of AgNPs using plant extracts which potentially retain some of their medicinal effects has become an attractive research endeavor. To date, numerous medicinal plants, such as *Cornus officinalis*,[32–35] Sea Buckthorn,[36] *Mentha*,[37–39] and Jujube[40] have been utilized to synthesize bioactive AgNPs.

Safflower (*Carthamus tinctorius* L.) is a member of the family Compositae or Asteraceae, whose medicinal properties have been known since ancient times and have been used for centuries.[41,42] In China, the flowers of safflower are widely used in Chinese herbal preparations due to their antioxidant, anti-inflammatory and antimicrobial properties, and they contain vitamins A and E, polyunsaturated fatty acids, linoleic acid, and other biologically active substances in large quantities.[43–46] The progression of some diseases like myopia (especially in children), trachoma, senile cataracts, symptoms of depression, cardiovascular disease and skin tumors have been successfully retarded by safflower or its mixtures with other herbs.[47,48] On the basis of its ingredients and medicinal effects, safflower has been used to fabricate bioactive AgNPs. For example, Kap Duk Lee and his coworker reported a green method for synthesizing AgNPs by using safflower flower extract.[49] The biosynthesized AgNPs showed inhibition effects against *E. coli*, *S. aureus*, *B. subtilis*, *C. albicans* and *B. cerevisiae* in both liquid and solid media. They also displayed significant cytotoxic effects on a human oral cancer cell line within the concentration range of 0.2 to 1.0 mM. Then, S. Najmeh Aboutorabi and his coworkers also biosynthesized AgNPs using safflower flower extract and evaluated the effects of process parameters, such as reaction time, temperature and extract solution concentration, on the properties of biosynthesized AgNPs and the antibacterial activity on applied wool fabric.[50] It is clear that the safflower flower could serve as a promising green resource to fabricate bioactive AgNPs.

To further exploit this sustainable resource, José Agustín Tapia-Hernández and his coworkers were recently concerned about safflower waste,[51] also called the non-medicinal parts, which accounted for about 80% of the plant. Their study aimed to biosynthesize AgNPs using an extract of mixed safflower leaf and stem, where the antibacterial activities of the AgNPs on *S. aureus* and *P. fluorescens* were disclosed with minimum inhibitory concentration (MIC) values of 1.9 and 7.8 μg mL^{-1}, respectively. One can well perceive that using the non-medicinal parts of safflower is a good choice for fabricating bioactive AgNPs. However, we noticed that in the pioneering study of José Agustín Tapia-Hernández and his coworkers, the AgNPs were generated after adding $AgNO_3$ solution and allowing it to stand for 12 h in the dark.[51] The relatively long reaction time and the strict reaction conditions may limit the application of this sustainable method. Otherwise, the mixture of leaf and stem was used as a green resource, but the ratio of these two parts was undefined, which has significant implications for the reproducibility of this green method. It is obvious that the efficiency of this reduction reaction should be improved and this pioneering method should be optimized.

Apart from safflower leaf and stem (SS), safflower bud (SB) is also a non-medicinal part and is always discarded in large quantities when preparing Chinese herbal medicines. It is anticipated that safflower bud could be regarded as a potential green resource for fabricating bioactive AgNPs.

In this study, pure SB and SS were selected as green resources for the sustainable biosynthesis of AgNPs with antioxidant, antibacterial and anticancer activities (Scheme 1). For the purpose of improving the efficiency of the reduction reaction, it was carried out with the assistance of ultrasonication and the

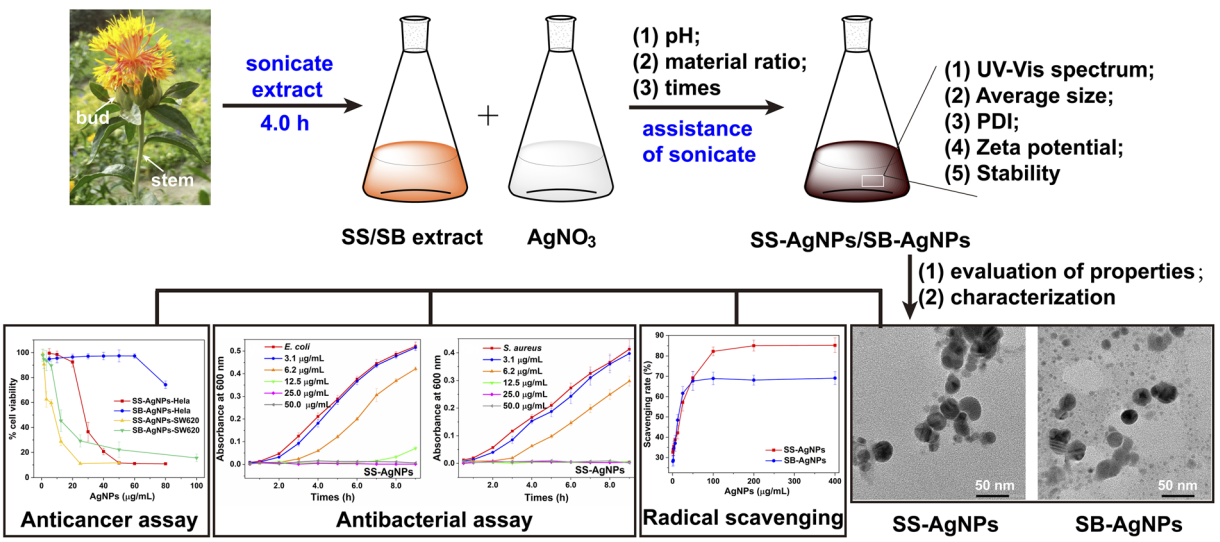

Scheme 1 Schematic representation of green synthesis, characterization, and biological activities of SS and SB mediated AgNPs.

biosynthesis parameters were optimized. The reduction reactions were monitored over time by visual observation and UV-vis spectroscopy accompanied by an evaluation of physicochemical properties like hydrodynamic diameter, polydispersity, zeta potential and stability under different process parameters. For biological applications, two kinds of AgNPs, named SS-AgNPs and SB-AgNPs, were biosynthesized after taking the effects of process parameters into full consideration. The morphology, crystalline nature and actual diameter of these two kinds of AgNPs were characterized by transmission electron microscopy (TEM), high-resolution transmission electron microscopy (HRTEM) and X-ray diffraction (XRD). Assays of radical scavenging were performed to disclose the antioxidant activity of both kinds of AgNPs. *E. coli* and *S. aureus* were applied as sensitive bacteria to evaluate the antibacterial properties *via* bacterial growth kinetic and minimum inhibitory concentration (MIC) analyses, where fluorescence staining experiments were used to illustrate the sterilization mechanism. The anticancer potentials of SS and SB mediated AgNPs against various human cancer cell lines were assessed thoroughly with an MTT assay. These results reveal that the assistance of ultrasonication and adjusting the process parameters are efficient methods for promoting the reduction reaction and both SS-AgNPs and SB-AgNPs could be treated as potential candidates for antioxidant, antibacterial and anticancer drugs.

2. Experimental

2.1 Materials

Safflower (dry) was collected from farmland located in Xinjiang Uygur Autonomous Region, China. The stem and bud were separated from safflower, respectively, and then ground to powder, and stored at room temperature for further studies. Silver nitrate ($AgNO_3$, 99.8%), sodium chloride, yeast powder, 1,1-diphenyl-2-picrylhydrazulin (DPPH, >99.5%), dimethyl sulfoxide (DMSO), 3-(4,5-dimethyl-2-thiazolyl)-2,5-diphenyl-2*H*-tetrazolium bromine (MTT), microorganisms and cancer cell lines used in this study were obtained as described in our previous studies.[52] All chemicals with analytical grade of purity were not enhanced further. Ultrapure Milli-Q water was used as a solvent and for washing.

2.2 Preparation of the extract and biosynthesis of AgNPs

10.0 g of the above ground powder for both safflower stem and bud was weighed and added to 100 mL of ultrapure water, and then the solution was ultrasonicated for 4.0 h at a frequency of 60 kHz. After this, the solution was filtered through filter paper. The resultant filtrates were collected and stored at 4 °C, to be treated as source extracts and utilized in subsequent experiments. The pH of the source extracts for safflower stem and bud are around 4 and 5, respectively.

$AgNO_3$ solution (10 mM) was prepared and used as the source of silver. The source extracts were added with a certain volume to 5.0 mL of the above-prepared $AgNO_3$ solution, where the total volume of the mixture was kept constant (10.0 mL). Sodium hydroxide (NaOH) was used to adjust the pH of the extract to the desired value. The complete mixtures were sonicated at room temperature, where their color changed from faint yellow to dark brown. Thereafter, the resultant dark brown mixtures were centrifuged at a high speed of 10 000 rpm for 30 min. After removing the supernatant, the precipitates were gathered and re-dispersed in ultrapure water three times to ensure the removal of extract residues and interactive biological molecules. Finally, the collected samples were lyophilized for 12 h.

2.3 Characterization of AgNPs

The presence of AgNPs was initially determined by measuring the UV-vis spectrum of the reaction medium after diluting a small aliquot of the sample with ultrapure water. The average size and polydispersity index (PDI) of the biosynthesized AgNPs were monitored by the dynamic light scattering (DLS) method. A zeta potential analyzer was used to obtain the ζ-potential of the AgNPs. Transmission electron microscopy (TEM, JEM-2100 Plus) was used for morphological characterization. Their crystalline nature was confirmed by high-resolution transmission electron microscopy (HRTEM) and X-ray diffraction (XRD, Bruker D8 Advance). The tube current and voltage of the X-ray diffractometer were set to 30 mA and 40 kV, respectively. The diffracted intensities were recorded at 2θ angles from 20° to 80° at a scanning rate of 5° per minute.

2.4 Antioxidant activity of AgNPs

A DPPH assay was conducted to evaluate the free radical scavenging activity of the AgNPs. 1.0 mL of AgNPs of different concentrations were first added to 1.0 mL of alcoholic DPPH solution (2.5 μg mL^{-1}). After vigorous shaking, the samples were incubated for 30 min in the dark at room temperature. The absorbance of DPPH at 517 nm, which was partially quenched due to the antioxidative AgNPs, was measured to calculate the scavenging percentage of free radicals. The scavenging percentage was obtained using the following formula:

$$\text{Scavenging rate } (\%) = [1 - (A_1 - A_2)/A_0] \times 100\%$$

where A_0 is the absorbance of DPPH in ethanol at 517 nm, A_1 is the absorbance of DPPH and AgNPs in ethanol at 517 nm, and A_2 is the absorbance of AgNPs in ethanol at 517 nm.

2.5 Antibacterial activity of AgNPs

The antibacterial activity of the biosynthesized AgNPs was evaluated on both Gram positive and negative bacteria, namely *S. aureus* and *E. coli*, respectively. The experiments were conducted in Luria–Bertani (LB) broth media and performed as per our previous study.[52] Briefly, twofold serial concentrations of AgNPs ranging from 0 to 100 μg mL^{-1} were first prepared, 50 μL of which were then inoculated with 50 μL of freshly prepared bacterial suspension in 96-well plates. The tested samples were incubated in a shaker incubator (160 rpm) at 37 °C for 24 h. The number of bacteria was counted every hour by measuring the absorbance of the bacteria at 600 nm. Plates with LB broth

media were used as a control, the absorbance of which were subtracted from each measurement.

The cell membrane disruption of both *S. aureus* and *E. coli* mediated by AgNPs was tested with DAPI and PI staining. The prepared bacterial suspension was treated with AgNPs (2*MIC) for 3 h. After washing with PBS, the bacteria were incubated with DAPI (5.0 μg mL^{-1}) and PI (10.0 μg mL^{-1}) for about 20 min in the dark, where the remaining dyes were washed off with PBS (×3). The controls without AgNP treatment were dyed using the same method described above.

2.6 Anticancer activity of AgNPs

Well-cultured HeLa and SW620 cell lines were plated out in flat-bottom 96-well plates at a density of 1×10^4 cells per well and allowed to attach for 24.0 h. After removal of the supernatant, twofold serial concentrations of AgNPs (0–100.0 μg mL^{-1}) were added into the test 96-well plates. They were cultured at 37 °C in an atmosphere of 5% CO_2 for 24.0 h. Then, 20 μL of thiazolyl blue tetrazolium bromide (MTT, 5.0 μg mL^{-1}) and 150 μL of DMEM medium were freshly added to each well. After 4.0 h of incubation, the media were gently removed to collect the formazan crystals, which were dissolved in 150 μL of DMSO followed by measurement of absorbance at 490 nm. The cell viability could be determined according to the following formula:

$$\text{Cell viability (\%)} = (A - A_b)/(A_0 - A_b) \times 100\%$$

where A is the absorbance of the test sample, A_b is the bleaching absorbance without the sample, and A_0 is the absorbance of the control.

3. Results and discussion

3.1 UV-vis spectroscopy

Initially, the source extracts of both safflower stem (SS, 5.0 mL) and bud (SB, 5.0 mL) were used as green sources for reducing silver ions (Ag^+, 5.0 mL) to Ag^0 with the assistance of ultrasonication. The successful synthesis of AgNPs was evidenced by a visual change in the color of the solution from faint yellow to brown within 3.0 h due to excitation of surface plasmon vibrations in AgNPs. The time of the color change was dramatically reduced in comparison with the previous study by using a mixture of safflower leaf and stem as the source extract,[51] indicating an accelerated reduction reaction under ultrasonic radiation. UV-vis spectroscopy, which is a well-established method to confirm the formation of AgNPs,[27] was used to analytically prove the reduced Ag^0 present in the SS and SB aqueous extract by observing the appearance of a surface plasmonic resonance (SPR) band in the range 400–500 nm. The absorption spectra of both SS and SB extracts alone showed no obvious peaks above 400 nm. After the reaction of SS with Ag^+, a new weak peak appeared in the interval of 400–500 nm attributable to AgNPs (SS-AgNPs, Fig. 1A). However, only a slight increase in absorbance in this interval was observed for the SB extract, which may be attributed to the very small amount of AgNPs in solution (SB-AgNPs, Fig. 1D). This result essentially agrees with visual observation of the color and indicates that the source extracts of both SS and SB are capable of reducing Ag^+ to Ag^0 but only with weak reduction. This is also consistent with a previous study reported by José Agustín Tapia-Hernández that AgNPs could be generated using a mixture of safflower leaf and stem after 12 h of incubation in the dark.[51]

To enhance the reducibility, the pH of both extracts was gradually adjusted from 4.0/5.0 to 10.0 and comparative experiments were performed at different pH. As shown in Fig. 1A, the absorption band of SS-AgNPs around 430 nm slightly decreased with increasing pH up to 7.0 and then greatly increased, where the maximum absorption was observed at pH 10.0. However, for SB-AgNPs, a continuously increasing absorption around 410 nm was observed (Fig. 1D). The increased absorption suggests the formation of more AgNPs and accelerated reduction. Peak locations of the plasmon absorption of AgNPs are affected by the size of the nanoparticles, with a shift to longer wavelength with increasing particle size. This indicates that the size of the generated SB-AgNPs is smaller than that of SS-AgNPs. Otherwise, on the basis of Mie's theory, spherical nanoparticles could give rise to only a single SPR band, whereas, according to the shape of the particles, two or more SPR bands are expected in the absorption spectra of anisotropic particles. Herein, the optical absorption spectra of both reaction mixtures displayed a single SPR band, revealing the spherical shape of the biosynthesized AgNPs, which was further confirmed by the TEM images. Since studies have documented that the AgNPs formed in more basic pH are unstable and agglomerate in the medium,[53] the pH of the extract was not adjusted further.

Reports indicated that the natural active ingredients in the extract not only reduce the metal ions to nanoparticles but also cover the formed nanoparticles by acting as capping agents.[25] Thus, the amounts of extract are considered to significantly influence the reduction of Ag^+ to Ag^0. In order to further accelerate the reduction, experiments were performed on different volume ratios of extract and $AgNO_3$ at pH 10.0. Fig. 1B and E display the optical absorption spectra of both SS and SB extracts with $AgNO_3$ after 4.0 and 6.0 h of incubation, respectively. With small amounts of extract (1 : 20), only a weak band with a maximum absorbance around 420 nm was observed. With a gradual increase in the amount of extract to 1 : 1, the absorption of the AgNPs around 420 nm increased significantly and reached a maximum. It is obvious that the greater the amount of extract added, the greater the number of AgNPs generated. This is consistent with previous studies. However, since both source extracts are so thick, extracts of larger concentration could not be obtained. In addition, the optical absorption spectra of these two mixtures in different material ratios also reveal the feature of a slight band shift, indicating various sizes of AgNPs.

Incubation time is also an important factor affecting the synthesis and stability of nanoparticles.[26] Fig. 1C and F display the UV-vis spectroscopy of the AgNPs after proximity to $AgNO_3$ with SS and SB extracts at different times, where the pH of both extracts is 10.0 and the material ratio is 1 : 1. It was found that after incubation for up to 4.0 h, the featured SPR band of AgNPs in both extracts could be clearly observed. With the passage of

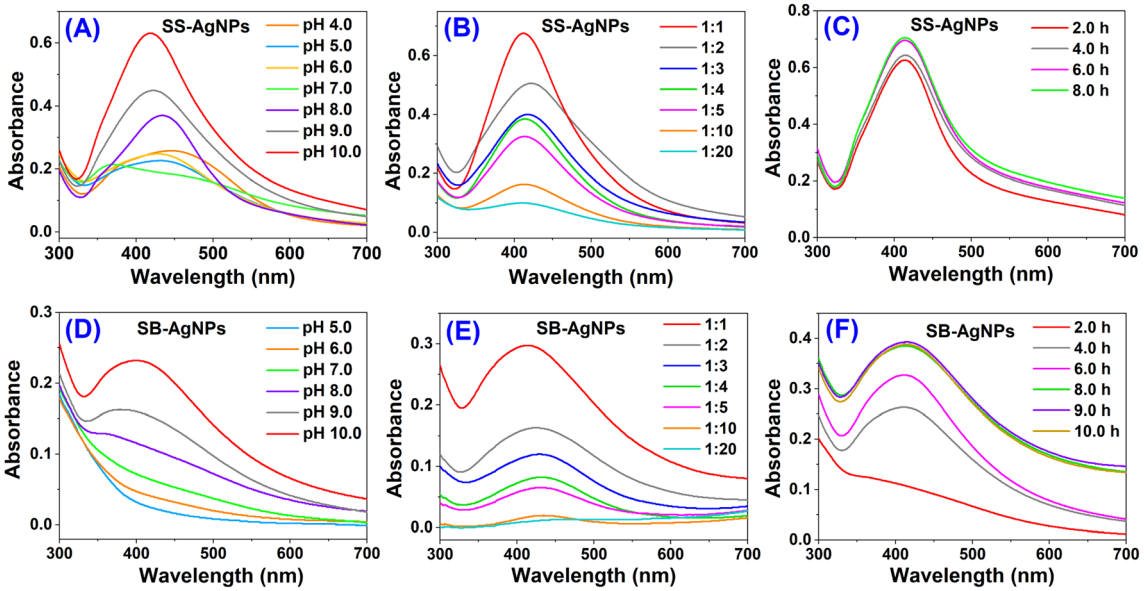

Fig. 1 UV-vis spectra of SS-AgNPs and SB-AgNPs obtained with different process parameters. (A) and (D) are at different pH; (B) and (E) have different material ratios; (C) and (F) have different incubation times.

time, the absorption of SS and SB mediated AgNPs rose steadily and reached a maximum after 6.0 and 8.0 h, respectively. After this, there were no obvious changes in the absorption associated with the AgNPs. The UV-vis spectra displayed a slight band shift within the incubation time, and the formation of AgNPs with different sizes should account for this. It is clear that the biosynthesis of AgNPs with 5.0 mL of 10 mM $AgNO_3$ and 5.0 mL of extract at pH 10.0 would show maximum efficiency and the reduction reaction would be fully completed within 6.0 and 8.0 h for SS and SB, respectively.

3.2 Average size

Size could determine the activity of nanoparticles in biomedical applications and thus is considered an important parameter. Previous reports indicated that the size of nanoparticles would be significantly influenced by the pH of the extract, which has a negligible effect on the shape.[30] Our earlier studies revealed that the average size of AgNPs is not necessarily the smallest under the conditions with maximum efficiency.[32,36,52] Thus, in order to obtain AgNPs with small size, the average size was measured by dynamic light scattering (DLS) when the material ratio of the extract and $AgNO_3$ was 1 : 1. DLS is an analytical method which estimates the particle diameter along with the external phytochemical coating, usually called the hydrodynamic diameter. The average sizes of the biosynthesized AgNPs at different pH after incubation for a certain time are shown in Fig. 2A and C. It is obvious that the average size of SS-AgNPs biosynthesized at pH 6.0 is relatively smaller than for other pH values and the smallest size of SS-AgNPs could be obtained at pH 8.0 after 6.0 h of incubation (19.7 ± 0.8 nm). However, this reveals that an alkaline solution could accelerate the generation of SB-AgNPs of small size. By adjusting the pH of the SB extract to 10.0, SB-AgNPs with the smallest average size (26.5 ± 1.5 nm) could be formed after 6.0 h of incubation. It should be noted that in acidic solution, AgNPs have a tendency to grow to larger size for both SS and SB. The distribution of average size is in accord with the evolution of the above-mentioned UV-vis spectrum.

Studies also showed that an optimum concentration of extract is necessary for the reduction and stabilization of nanoparticles.[29] If the concentration is outside this level, the nanoparticles are obtained in lower amounts and with a bulkier size or they accumulate, causing defective stabilization and coarser particles. Thus, the effects of the material ratio on the average size of SS and SB mediated AgNPs were assessed at pH 10.0 after 4.0 and 6.0 h of incubation, respectively. The results are displayed in Fig. 2B and D. With increased concentration of

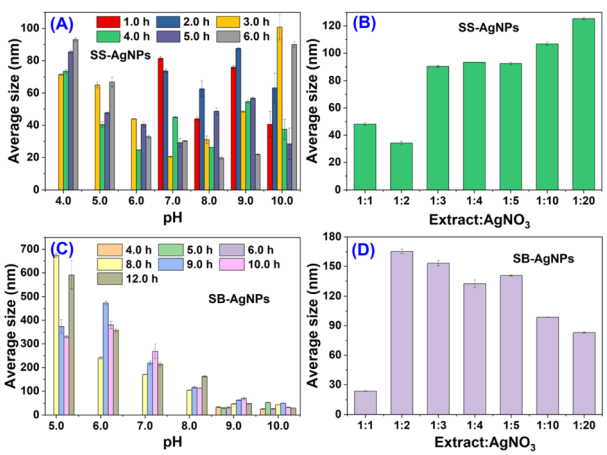

Fig. 2 Hydrodynamic diameters of SS-AgNPs and SB-AgNPs obtained for different process parameters. (A) and (C) have different pH and incubation times; (B) and (D) have different material ratios.

extract, the average sizes of the AgNPs biosynthesized by SS and SB show different variation tendencies. The average size of SS-AgNPs gradually decreased and reached a minimum when the ratio was 1 : 2. However, there was an increase in average size until the concentration of the SB extract reached 1 : 2. When the ratio was adjusted to 1 : 1, the average size dramatically decreased to 23.5 ± 0.3 nm.

3.3 Polydispersity

Polydispersity is another important parameter for nanoparticles, which has a significant effect on the characteristics of nanoparticles. Thus, the polydispersity index (PDI) of AgNPs biosynthesized by both SS and SB was determined. Fig. 3A and C display the PDI of AgNPs obtained when the material ratio was 1 : 1 for both extracts. They show that SS-AgNPs with the smallest and largest PDI values could be generated at pH 4.0 and 7.0, respectively. A neutral solution is disadvantageous to the generation of SS-AgNPs with superior dispersion. The smallest PDI value of SS-AgNPs is 0.22 ± 0.01. However, a neutral SB extract facilitates the generation of AgNPs with superior dispersion. SB-AgNPs in neutral solution have smaller PDI values compared with those synthesized in alkaline or acidic solutions. The smallest PDI value (0.27 ± 0.01) was obtained when the experiment was performed at pH 8.0 after 8.0 h of incubation. Studies indicated that, if the sample has a PDI value lower than 0.3, it would exist in monodispersed form. Herein, the smallest PDI values of SS-AgNPs and SB-AgNPs are below this level, indicating that AgNPs with superior dispersion could be generated by both SS and SB extracts.

The effect of the material ratio on the PDI of the AgNPs was also evaluated when the experiment was performed at pH 10.0 after 4.0 and 6.0 h of incubation with SS and SB, respectively. It is obvious that, with increased concentration, the PDI of SS-AgNPs gradually increases. The smallest PDI (0.19 ± 0.02) could be obtained when the material ratio was 1 : 20. The high concentration of SB extract (1 : 1) would form SB-AgNPs with poor dispersion, where the PDI value was 0.82 ± 0.01. With other material ratios used in this study, the PDI of AgNPs is below the value of 0.3, meaning accessibility to AgNPs with superior dispersion.

3.4 ζ-Potential

ζ-Potential is a physicochemical property that is associated with the stability of nanoparticles and it has a significant effect on antimicrobial activity, since electrostatic adhesion would facilitate the interaction of nanoparticles and the cell membrane.[27] It is well known that particles with higher repulsive forces demonstrate robust Brownian movement with greater stability. In parallel, particles with increased attractive forces aggregate and settle down, and may fail to demonstrate biological activities. Clearly, nanoparticles with a high magnitude of ζ-potential are electrically stable, while nanoparticles with a low magnitude of ζ-potential tend to coagulate. Previous studies indicated that nanoparticles with ζ-potentials in the interval −25.0 to +25.0 mV may lead to the aggregation of nanoparticles deriving from interparticle attraction. However, if the ζ-potentials are outside of this range, the nanoparticles would show long-term stability. Therefore, the ζ-potential was measured to judge the surface state and the stability of the AgNPs synthesized by both extracts. Fig. 4A compares the ζ-potential of AgNPs synthesized by SS and SB extracts at different pH when the material ratio was 1 : 1 after 5.0 and 8.0 h of incubation, respectively. Obviously, the SS-AgNPs have larger ζ-potential values than the SB-AgNPs, meaning greater loads on the surface of SS-AgNPs. For both SS

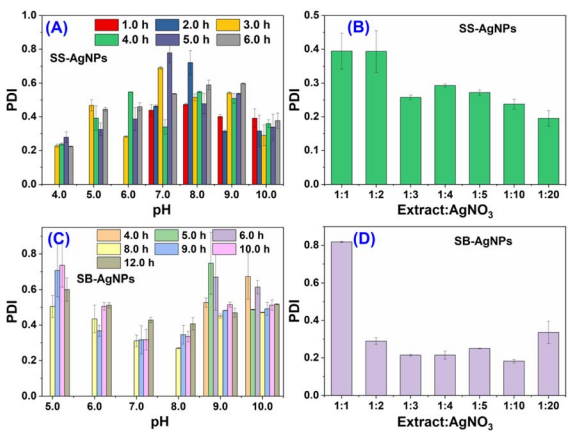

Fig. 3 Polydispersity index (PDI) of SS-AgNPs and SB-AgNPs obtained with different process parameters. (A) and (C) have different pH and incubation times; (B) and (D) have different material ratios.

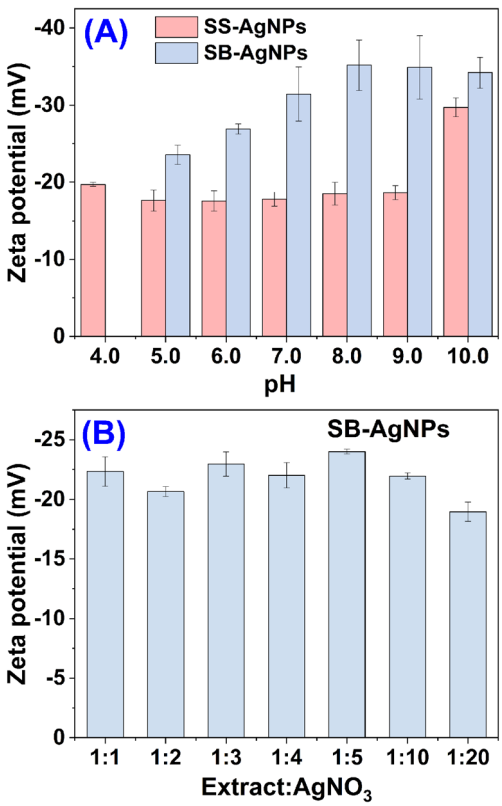

Fig. 4 The ζ-potential of AgNPs obtained at different (A) pH; (B) material ratios.

and SB, a basic solution facilitates the generation of more loaded AgNPs. The largest ζ-potential value of SS and SB capped AgNPs were −29.7 ± 1.2 and −35.2 ± 3.2 mV at pH 10.0 and 8.0, respectively, indicating a high degree of stability. In practice, when the synthetic AgNPs were left for 30 days, the average size revealed negligible change, verifying their superior stability. Otherwise, the negative ζ-potential means electronegative capping agents on the surface of the AgNPs. These molecules may be flavonoids, tannins, proteins, polysaccharides, steroids, fatty acids, phenolic acids, anthocyanins, or gallic acid derivatives contained in the SS and SB extracts, as confirmed by previous FTIR studies by José Agustín Tapia-Hernández and his coworkers.[51]

Fig. 4B displays the ζ-potential of synthetic AgNPs with various concentrations of SB extract at pH 10.0 after 8.0 h of incubation. It was anticipated that the greater the amount of extract added, the greater the load would be on the surface of the AgNPs. However, the material ratio seems to have a negligible effect on the ζ-potential of the synthetic AgNPs.

In order to obtain more AgNPs of small size for further characterization and investigations of biological activity, reduction reactions were performed at pH 10.0 and material ratio 1 : 1 for both SS and SB extracts, where the reaction mixtures were incubated for 5.0 h and 6.0 h, respectively.

3.5 EDS, TEM and XRD

Elemental analysis (EDS) was used to confirm the generation of AgNPs after incubating both SS and SB extracts with Ag^+ under certain biosynthesis parameters. As shown in Fig. 5, both SS-AgNPs and SB-AgNPs display a strong absorption peak around 3 keV, which originates mainly from elemental silver, verifying the existence of Ag^0. Another two strong signals resulting from carbon and copper in the spectrum should relate to the carbon-coated copper grid used in the TEM and EDS analysis. The weak signals originating from S, Cl, P, *etc.* should be assigned to the capping agents of AgNPs, which were predicted to be proteins, polysaccharides/sugars and phenolic compounds, mainly flavonoids, by a previous FTIR experiment, as mentioned above.[51]

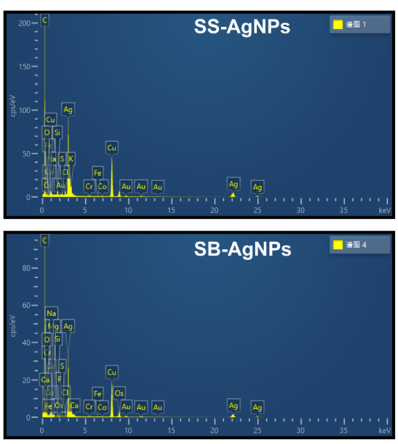

Fig. 5 EDS patterns of biosynthesized SS-AgNPs and SB-AgNPs.

TEM was used to visualize the actual particle size and the overall size distribution, which are fundamental measures to investigate the repeatability and efficiency of various processes aimed at the synthesis of nanoparticles. As shown in Fig. 6A and C, the SS and SB mediated AgNPs are mainly monodispersed with little aggregation, basically in accord with the above PDI analysis. The shapes of the SS-AgNPs and SB-AgNPs are both spherical, reinforced by the sharp and narrow peak of the UV-visible spectrum in Fig. 1. It is obvious that the SS-AgNPs have diameters roughly in the range of 20–30 nm basically in accordance with the DLS results. The diameters of the SS-AgNPs are slightly bigger than those of SB-AgNPs, which appear to be below 20 nm. The morphological properties of the AgNPs synthesized here agree with those synthesized from a mixture of safflower leaf and stem.[51]

Fig. 6B and D display the HRTEM images, which reveal lattice fringes, clearly indicating the crystalline nature of both kinds of AgNP. The lattice fringes were measured to be 1.083 Å and 1.499 Å for SS-AgNPs and SB-AgNPs, respectively, which may originate from the characteristic reflections of cubic and hexagonal crystalline silver. To further illustrate their crystalline structure, X-ray diffraction (XRD) experiments were performed and the results are displayed in Fig. 7. The typical peaks observed for both SS-AgNPs and SB-AgNPs are almost the same, indicating the same crystalline structure. The Bragg's diffraction peaks appearing at 38.27°, 44.30°, 64.58°, and 77.48° correspond to the (111), (200), (220) and (311) facets of cubic Ag, indicating a face-centered cubic (fcc) crystalline structure. Hexagonal Ag with 2θ angles of 46.14°, 54.79°, 57.63°, 64.58°, 67.43° and 76.78° corresponding to (103), (006), (105), (110), (112) and (201) facets were also observed. The XRD pattern clearly showed the presence of crystalline structures (cubic and hexagonal) for both AgNPs and confirmed that the SS and SB

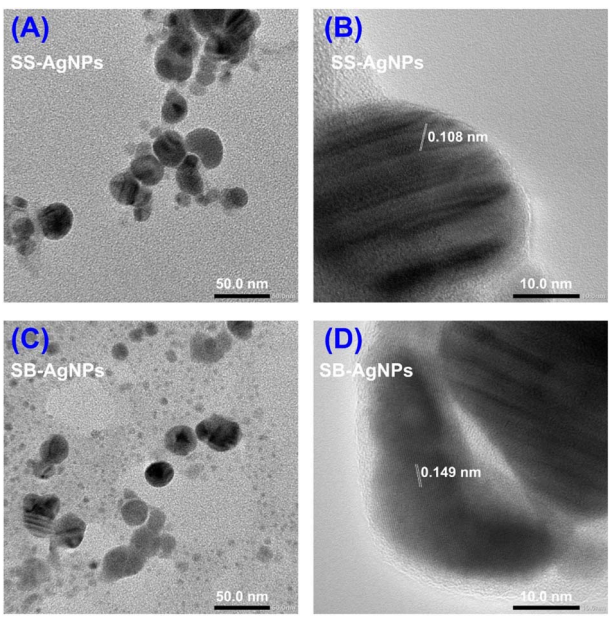

Fig. 6 (A) TEM image and (B) HRTEM image of SS-AgNPs; (C) TEM image and (D) HRTEM image of SB-AgNPs.

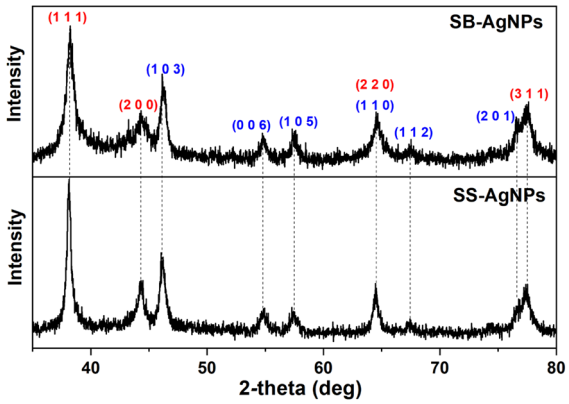

Fig. 7 XRD patterns of SS-AgNPs and SB-AgNPs.

extracts could reduce the Ag^{+} to AgNPs. Furthermore, no other apparent phases were observed in the XRD patterns, indicating the high purity of the SS-AgNPs and SB-AgNPs.

3.6 Antioxidant activities

Based on previous studies, safflower contains more than 200 species, such as a high content of flavonoids and polyphenols in the aqueous extract.[41] Several authors have documented the antioxidant activity of safflower extract and the essential oils originating from safflower.[54] As AgNPs would be coated by the bioactive constituents involved in SS and SB extracts, the SS and SB mediated AgNPs are anticipated to exhibit potent antioxidant activity. Thus, a DPPH assay was performed to evaluate the antioxidant activity of biosynthesized AgNPs, which is one of the quickest methods. DPPH is a stable free radical, and its color changes from purple to yellow when it accepts hydrogen and electrons from donors.

The rates of free radical scavenging were calculated after adding twofold serial concentrations of synthetic AgNPs into DPPH solution. As shown in Fig. 8, the AgNPs capped by SS and SB reveal significant DPPH scavenging activity, which is closely related to the concentration of synthetic AgNPs. When the concentration of AgNPs synthesized by SS was increased from 0.78 to 100 μg mL^{-1}, the scavenging activities increased from 32.6% to 82.2%. Further addition of AgNPs to 400 μg mL^{-1} had only a small influence on the radical scavenging activities (85.2%). The scavenging activity of AgNPs capped by SB is smaller than that for SS-AgNPs. The SB-AgNPs had scavenging activity of 67.7% in 50.0 μg mL^{-1}. However, when the amount of AgNPs was increased to 400.0 μg mL^{-1}, the scavenging activity changed slightly to 69.1%. Herein, the radical scavenging activity of AgNPs capped by SS and SB is comparable with those from previous reports[55,56] indicating their potential application in the treatment of many diseases caused by oxidative stress.

3.7 *In vitro* antibacterial activities

The growth kinetics of *E. coli* and *S. aureus* were measured for the purpose of evaluating the antibacterial activities of synthetic AgNPs. After treatment with twofold serial concentrations of AgNPs, the absorbance of bacteria at 600 nm was measured and is displayed in Fig. 9, exhibiting dose-dependence. Growth inhibition could obviously be observed for both pathogens, even when treated with 3.1 μg mL^{-1} AgNPs synthesized with both extracts. For SS mediated AgNPs, the minimum inhibition concentrations (MICs) were found to be 25.0 and 12.5 μg mL^{-1} against *E. coli* and *S. aureus*, respectively. However, when these two pathogens were incubated with SB-AgNPs, the MICs were determined to be 25.0 and 50.0 μg mL^{-1}, a little bit higher than for SS mediated AgNPs. The MIC of AgNPs obtained herein is slightly different from those obtained by José Agustín Tapia-Hernandez using wastage from safflower (*S. aureus* 1.9 μg mL^{-1}; *P. fluorescens* 7.8 μg mL^{-1}).[51] We speculate that the difference might arise from the different methods used for the assessment of antibacterial activity and the AgNPs having different physicochemical properties.

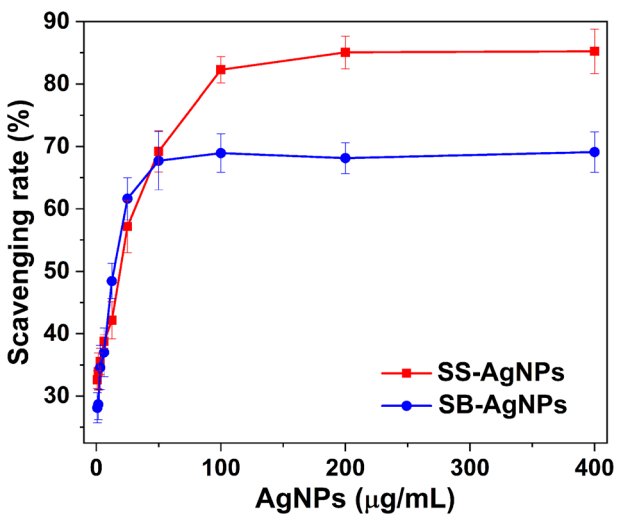

Fig. 8 Free radical scavenging rate of AgNPs against DPPH.

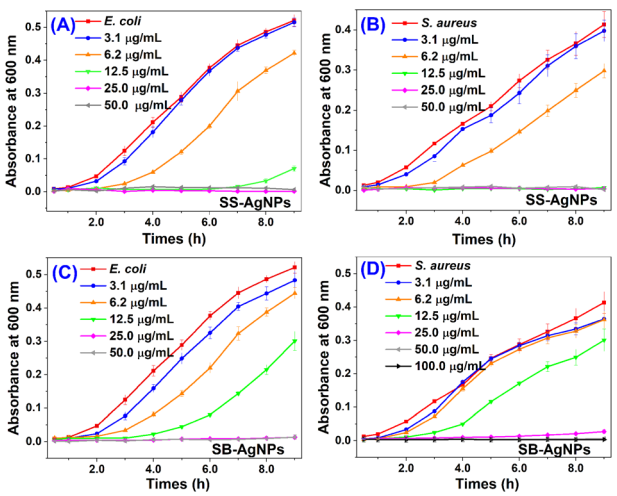

Fig. 9 The antibacterial activity of SS-AgNPs for (A) *E. coli* and (B) *S. aureus* and of SB-AgNPs for (C) *E. coli* and (D) *S. aureus*.

To illustrate the sterilization mechanism of biosynthesized AgNPs, fluorescence staining experiments labeling the live/dead bacteria cells with DAPI and PI were performed, where DAPI stains all bacteria regardless of the viability of the cells but PI stains only specific cells with damaged membranes. As shown in Fig. S1,† the bacterial cells without AgNPs treatment were stained by DAPI, showing blue fluorescence, but not by PI, indicating that the bacterial membranes were intact. However, after treatment with AgNPs (2*MIC), both types of bacterial cell were stained by PI, showing red fluorescence, verifying that the membranes of both cells had been disrupted.

3.8 *In vitro* anticancer activities

Apart from combatting infections, AgNPs are also used to deal with serious health problems such as cancer, especially multi-drug resistant cancer cells.[27] Herein, an MTT assay was performed to evaluate the anticancer activity of both SS and SB mediated AgNPs against human colorectal cancer SW620 and cervical cancer HeLa *in vitro*. As shown in Fig. 10, the incubation of these two cancer lines with SS mediated AgNPs would give rise to a decrease in cell viability in a dose-dependent fashion. With the addition of 50 μg mL^{-1} SS-AgNPs, the cell viabilities of SW620 and HeLa were significantly reduced to 11.0% and 11.6%, respectively. The AgNPs synthesized by SB also display cytotoxicity against the SW620 cell line, where the cell viability was found to be 22.2% at 50 μg mL^{-1} SB-AgNPs. Interestingly, they seem to be incapable of action against the HeLa cell line even after treatment with 80 μg mL^{-1} SB-AgNPs.

To further evaluate the results of the anticancer assay, the half-maximal inhibitory concentration (IC_{50}) of the AgNPs is presented, which represents a quantitative measure of the drug concentration required to inhibit a certain biological process by half. By fitting the dose–response curve constructed above, the IC_{50} values of the AgNPs against cancer cell lines were determined to be 5.4 (SS-SW620), 10.6 (SB-SW620) and 26.8 μg mL^{-1} (SS-HeLa). These results demonstrated the potential anticancer activity of AgNPs against cancer cell lines with varying sensitivity.

The AgNPs synthesized by SS and SB extracts herein displayed high anticancer activity, comparable with AgNPs synthesized using Iranian *Mentha pulegium* (~100 μg mL^{-1} for HeLa and MCF-7),[37] *Iresine herbstii* (51 μg mL^{-1} for HeLa)[57] and *Cornus officinalis* (20.68 and 69.72 μg mL^{-1} for HCT116 and HepG2, respectively),[32] and *Sea Buckthorn* (8.77, 14.59, and 27.98 μg mL^{-1} for HCT116, HepG2, and HeLa, respectively).[36] This means that the AgNPs synthesized herein could be regarded as promising candidates for anticancer drugs.

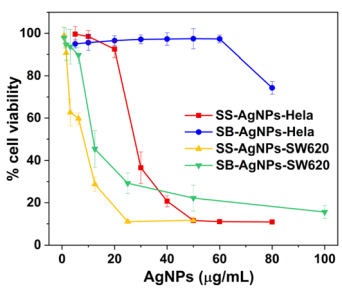

Fig. 10 Inhibition effects of AgNPs on SW620 and HeLa cell lines.

4. Conclusions

In the present study, AgNPs were produced by a sustainable green chemistry method with the non-medicinal parts of safflower (pure bud and stem) as potent bioreducers with the assistance of sonication. The current method of biosynthesis using safflower stem and bud is more time-efficient and resource-efficient, taking into account both the safety design and the needs of biological action and could be pursued in a wide range of contexts. By employing our established method, AgNPs with desirable particle sizes and stability characteristics could be conveniently generated by adjusting process parameters like the pH of the extract, the material ratio and incubation time. Characterization of the selectively synthesized AgNPs revealed their crystalline structure, average size, and surface loads. The antioxidant potentials of as-prepared AgNPs were disclosed by a radical scavenging experiment. An *in vitro* antibacterial and anticancer assay of both kinds of AgNPs demonstrated dose-dependent action in a certain concentration range against both pathogens and cancer cell strains, confirming their potent biological activity. The results of the present study provide experimental evidence that the assistance of sonication and adjusting the process parameters are efficient methods for promoting the reduction reaction, and that both SS and SB mediated AgNPs could serve as promising antioxidant, antibacterial and anticancer agents.

Conflicts of interest

There are no conflicts to declare.

Acknowledgements

This work was financially supported by the National Natural Science Foundation of China (Grant No. 82274353, 22103007); Key Scientific Research Plan of Shaanxi Provincial Department of Education (Grant No. 21JY009); Natural Science Foundation of Shaanxi Province (Grant No. 2021JQ-221); Xi'an Science and Technology Plan Project (Grant No. 22GXFW0153); Open Foundation of Shaanxi University of Chinese Medicine Key Laboratory of Research & Development of Characteristic Qin Medicine Resources (Grant No. SUCM-QM202207) and the Fundamental Research Funds for the Central Universities, CHD (Grant No. 300102122110).

Notes and references

1 B. Bhattarai, Y. Zaker, A. Atnagulov, B. Yoon, U. Landman and T. P. Bigioni, *Acc. Chem. Res.*, 2018, **51**, 3104–3113.
2 S. A. Khan, M. Jain, A. Pandey, K. K. Pant, Z. M. Ziora, M. A. T. Blaskovich, N. P. Shetti and T. M. Aminabhavi, *J. Environ. Manage.*, 2022, **319**, 115675.
3 F. Lu, *Coord. Chem. Rev.*, 2022, **456**, 214363.

4 S. Chatterjee, X. Y. Lou, F. Liang and Y. W. Yang, *Coord. Chem. Rev.*, 2022, **459**, 214461.
5 P. S. Araujo, M. B. Caixeta, A. Canedo, E. D. Nunes, C. Monteiro and T. L. Rocha, *Sci. Total Environ.*, 2022, **834**, 155299.
6 S. K. Chandraker and R. Kumar, *Biotechnol. Genet. Eng. Rev.*, 2022, DOI: **10.1080/02648725.2022.2106084**.
7 Y. H. Yang, S. Duan and H. Zhao, *Nanoscale*, 2022, **14**, 11484–11511.
8 Y. Yu, Z. Zhou, G. Huang, H. Cheng, L. Han, S. Zhao, Y. Chen and F. Meng, *Water Res.*, 2022, **222**, 118901.
9 F. Mo, Q. X. Zhou and Y. Q. He, *Sci. Total Environ.*, 2022, **829**, 154644.
10 M. Khubchandani, N. R. Thosar, S. Dangore-Khasbage and R. Srivastava, *Cureus*, 2022, **14**, e26956.
11 G. Pasparakis, *Wiley Interdiscip. Rev.: Nanomed. Nanobiotechnol.*, 2022, e1817.
12 A. Abbas and H. M. A. Amin, *Microchem. J.*, 2022, **175**, 107166.
13 R. K. Sharma, S. Yadav, S. Dutta, H. B. Kale, I. R. Warkad, R. Zboril, R. S. Varma and M. B. Gawande, *Chem. Soc. Rev.*, 2021, **50**, 11293–11380.
14 K. Kalantari, E. Mostafavi, A. M. Afifi, Z. Izadiyan, H. Jahangirian, R. Rafiee-Moghaddam and T. J. Webster, *Nanoscale*, 2020, **12**, 2268–2291.
15 S. M. Ghoreishian, S. M. Kang, G. S. R. Raju, M. Norouzi, S. C. Jang, H. J. Yun, S. T. Lim, Y. K. Han, C. Roh and Y. S. Huh, *Chem. Eng. J.*, 2019, **360**, 1390–1406.
16 P. Slepicka, N. S. Kasalkova, J. Siegel, Z. Kolska and V. Svorcik, *Materials*, 2020, **13**, 1.
17 N. Jara, N. S. Milan, A. Rahman, L. Mouheb, D. C. Boffito, C. Jeffryes and S. A. Dahoumane, *Molecules*, 2021, **26**, 4585.
18 K. Cubova and V. Cuba, *Radiat. Phys. Chem.*, 2020, **169**, 108774.
19 C. Iriarte-Mesa, Y. C. Lopez, Y. Matos-Peralta, K. de la Vega-Hernandez and M. Antuch, *Top. Curr. Chem.*, 2020, **378**, 12.
20 N. B. Abramenko, T. B. Demidova, E. V. Abkhalimov, B. G. Ershov, E. Yu. Krysanov and L. M. Kustov, *J. Hazard. Mater.*, 2018, **347**, 89–94.
21 G. R. Tortella, O. Rubilar, N. Duran, M. C. Diez, M. Martinez, J. Parada and A. B. Seabra, *J. Hazard. Mater.*, 2020, **390**, 121974.
22 S. Jadoun, N. P. S. Chauhan, P. Zarrintaj, M. Barani, R. S. Varma, S. Chinnam and A. Rahda, *Environ. Chem. Lett.*, 2022, **20**, 3153–3197.
23 A. Ullah and S. I. Lim, *Biotechnol. Bioeng.*, 2022, **119**, 2273–2304.
24 M. Alavi, *Expert Rev. Anti-Infect. Ther.*, 2022, **20**, 897–906.
25 C. Vanlalveni, S. Lallianrawna, A. Biswas, M. Selvaraj, B. Changmai and S. L. Rokhum, *RSC Adv.*, 2021, **11**, 2804–2837.
26 H. R. El-Seedi, R. M. El-Shabasy, S. A. M. Khalifa, A. Saeed, A. Shah, R. Shah, F. J. Iftikhar, M. M. Abdel-Daim, A. Omri, N. H. Hajrahand, J. S. M. Sabir, X. B. Zou, M. F. Halabi, W. Sarhan and W. S. Guo, *RSC Adv.*, 2019, **9**, 24539–24559.
27 K. Jadhav, S. Deore, D. Dhamecha, H. R. Rajeshwari, S. Jagwani, S. Jalalpure and R. Bohara, *ACS Biomater. Sci. Eng.*, 2018, **4**, 892–899.
28 M. Alavi, N. Karimi and T. Valadbeigi, *ACS Biomater. Sci. Eng.*, 2019, **5**, 4228–4243.
29 S. B. Ulaeto, G. M. Mathew, J. K. Pancrecious, J. B. Nair, T. P. D. Rajan, K. K. Maiti and B. C. Pai, *ACS Biomater. Sci. Eng.*, 2020, **6**, 235–245.
30 N. Tarannum, Divya and Y. K. Gautam, *RSC Adv.*, 2019, **9**, 34926–34948.
31 A. Roy, O. Bulut, S. Some, A. K. Mandal and M. D. Yilmaz, *RSC Adv.*, 2019, **9**, 2673–2702.
32 Y. Wang, S. Wei, K. Wang, Z. Wang, J. Duan, L. Cui, H. Zheng, Y. Wang and S. Wang, *RSC Adv.*, 2020, **10**, 27173–27182.
33 S. M. Wei, Y. H. Wang, Z. S. Tang, R. Su, J. H. Hu, H. Guo, C. Li, J. T. Jiang and Z. X. Song, *Chem. J. Chin. Univ.*, 2020, **41**, 1391–1398.
34 Y. He, X. Li, J. Wang, Q. Yang, B. Yao, Y. Zhao, A. Zhao, W. Sun and Q. Zhang, *Environ. Toxicol. Pharmacol.*, 2017, **56**, 56–60.
35 S. Wei, Z. Tang, H. Li, K. Zhang and Z. Song, *Chin. Tradit. Herb. Drugs*, 2019, **50**, 52–58.
36 S. M. Wei, Y. H. Wang, Z. S. Tang, J. H. Hu, R. Su, J. J. Lin, T. Zhou, H. Guo, N. Wang and R. R. Xu, *New J. Chem.*, 2020, **44**, 9304–9312.
37 Y. H. Wang and S. M. Wei, *ACS Omega*, 2022, **7**, 1494–1504.
38 M. Gholami, F. Azarbani and F. Hadi, *Mater. Technol.*, 2022, **37**, 934–942.
39 A. H. Abd Kelkawi, A. A. Kajani and A. K. Bordbar, *IET Nanobiotechnol.*, 2017, **11**, 370–376.
40 S. Wei, Y. Wang, Z. Tang, R. Su, H. Xu, L. Chen, S. Liu and C. Li, *Nat. Prod. Res. Dev.*, 2020, **32**, 182–190.
41 J. Asgarpanah and N. Kazemivash, *Chin. J. Integr. Med.*, 2013, **19**, 153–159.
42 I. Adamska and P. Biernacka, *J. Food Sci.*, 2021, **2021**, 6657639.
43 X. D. Zhou, L. Y. Tang, Y. L. Xu, G. H. Zhou and Z. J. Wang, *J. Ethnopharmacol.*, 2014, **151**, 27–43.
44 Z. Abuova, A. Turgumbayeva, A. Jumagaziyeva, K. Rakhimov and A. Jussupkaliyeva, *Int. J. Microbiol.*, 2022, **2022**, 3181270.
45 A. A. Turgumbayeva, G. O. Ustenova, B. K. Yeskalieva, B. A. Ramazanova, K. D. Rahimov, H. Aisa and K. T. Juszkiewicz, *Ann. Agric. Environ. Med.*, 2018, **25**, 87–89.
46 X. Y. Wu, X. B. Cai, J. X. Ai, C. Zhang, N. Liu and W. Gao, *Front. Pharmacol.*, 2021, **12**, 767947.
47 W. Toma, L. L. Guimaraes, A. Brito, A. R. Santos, F. S. Cortez, F. H. Pusceddu, A. Cesar, L. S. Junior, M. T. T. Pacheco and C. D. S. Pereira, *Rev. Bras. Farmacogn.*, 2014, **24**, 538–544.
48 A. Turgumbayeva, G. Ustenova, U. Datkhayev, K. Rahimov, S. Abramavicius, A. Tunaityte, K. Zhakipbekov, K. Kozhanova, S. Tulemissov, O. Ustenova, G. Datkayeva and E. Stankevicius, *Phyton-Int. J. Exp. Bot.*, 2020, **89**, 137–146.
49 T. V. M. Sreekanth and K. D. Lee, *Curr. Nanosci.*, 2011, **7**, 1046–1053.

50 S. N. Aboutorabi, M. Nasiriboroumand, P. Mohammadi, H. Sheibani and H. Barani, *J. Inorg. Organomet. Polym.*, 2018, **28**, 2525–2532.
51 F. Rodriguez-Felix, A. G. Lopez-Cota, M. J. Moreno-Vasquez, A. Z. Graciano-Verdugo, I. E. Quintero-Reyes, C. L. Del-Toro-Sanchez and J. A. Tapia-Hernandez, *Heliyon*, 2021, **7**, e06923.
52 S. M. Wei, Y. H. Wang, Z. S. Tang, H. B. Xu, Z. Wang, T. Yang and T. Y. Zou, *RSC Adv.*, 2021, **11**, 1411–1419.
53 S. Khan, S. Singh, S. Gaikwad, N. Nawani, M. Junnarkar and S. V. Pawar, *Environ. Sci. Pollut. Res. Int.*, 2019, **27**, 27221–27233.
54 X. X. Zhao, Y. He, Y. Y. Zhang, H. F. Wan, H. T. Wan and J. H. Yang, *Oxid. Med. Cell. Longevity*, 2022, **2022**, 1425369.
55 F. O. Kup, S. Coskuncay and F. Duman, *Mater. Sci. Eng., C*, 2020, **107**, 11.
56 T. Fafal, P. Taştan, B. S. Tüzün, M. Ozyazici and B. Kivcak, *Afr. J. Bot.*, 2017, **112**, 346–353.
57 C. Dipankar and S. Murugan, *Colloids Surf., B*, 2012, **98**, 112–119.